

# Design and Experimental Evaluation of Cooperative Adaptive Cruise Control

Jeroen Ploeg, Bart T. M. Scheepers, Ellen van Nunen, Nathan van de Wouw, Henk Nijmeijer

**Abstract**—Road throughput can be increased by driving at small inter-vehicle time gaps. The amplification of velocity disturbances in upstream direction, however, poses limitations to the minimum feasible time gap. String-stable behavior is thus considered an essential requirement for the design of automatic distance control systems, which are needed to allow for safe driving at time gaps well below 1 s. Theoretical analysis reveals that this requirement can be met using wireless inter-vehicle communication to provide real-time information of the preceding vehicle, in addition to the information obtained by common Adaptive Cruise Control (ACC) sensors. In order to validate these theoretical results and to demonstrate the technical feasibility, the resulting control system, known as Cooperative ACC (CACC), is implemented on a test fleet consisting of six passenger vehicles. Experiments clearly show that the practical results match the theoretical analysis, thereby indicating the possibilities for short-distance vehicle following.

## I. INTRODUCTION

In recent years, highway capacity has become a limiting factor, regularly causing traffic jams. Obviously, the road capacity can be increased by decreasing the inter-vehicle distance while maintaining the same velocity level. As a consequence, however, vehicle automation in longitudinal direction is required in order to still guarantee safety. To this end, Adaptive Cruise Control (ACC) seems to be an option. ACC automatically adapts the velocity of a vehicle so as to realize a desired distance to the preceding vehicle, or, in the absence of one, realizes a desired velocity. The inter-vehicle distance and the relative velocity are measured by means of a radar or a scanning laser (lidar). However, ACC is primarily intended as a comfort system. Consequently, relatively large inter-vehicle distances are adopted [1], with a standardized minimum of 1 s time headway [2], the latter referring to the geometric distance divided by the vehicle velocity.

Decreasing the time headway to a value significantly smaller than 1 s, is expected to yield an increase in traffic throughput [3]. Moreover, a significant reduction in the aerodynamic drag force is possible in case of heavy-duty vehicles, thereby decreasing fuel consumption and emissions [4]. It has however been shown that the application of ACC amplifies disturbances in upstream direction at small time gaps, see, e.g., [5] and the literature references contained therein. These disturbances may, e.g., be induced by velocity variations of the first vehicle in a string of vehicles. As

This work is funded by the Dutch Ministry of Economic Affairs through the High Tech Automotive Systems (HTAS) program, grant HTASD08002.

J. Ploeg, B. T. M. Scheepers and E. van Nunen are with TNO, P.O. Box 756, 5700 AT Helmond, The Netherlands, jeroen.ploeg@tno.nl, bart.scheepers@tno.nl, ellen.vannunen@tno.nl

N. van de Wouw and H. Nijmeijer are with the Eindhoven University of Technology, Mechanical Engineering Department, Eindhoven, The Netherlands, n.v.d.wouw@tue.nl, h.nijmeijer@tue.nl



Fig. 1. Test fleet, consisting of CACC-equipped passenger vehicles.

a result, fuel consumption and emissions increase, and so-called ghost traffic jams may occur, negatively influencing throughput whereas safety might be compromised as well.

Disturbance attenuation across the vehicle string is therefore an essential requirement, to be achieved by appropriately designed vehicle following controllers. The disturbance evolution across a string of vehicles, or, in general, across a number of interconnected subsystems, is covered by the notion of *string stability*, where string-stable behavior refers to the attenuation of disturbances in upstream direction. Application of data exchange by means of wireless communication in addition to the data obtained by radar or lidar, is known to be able to achieve string stability [5]. The resulting functionality is called Cooperative ACC (CACC). A vast amount of literature focussing on control design for CACC systems is available, see, e.g., [5]–[10]. The focus is, however, often on theoretical analysis rather than on the practical implementation and the evaluation thereof.

This paper, therefore, focusses on the practical implementation of CACC, using a test set-up consisting of six passenger vehicles as depicted in Fig. 1. To this end, the next section first provides a short overview of string stability concepts. Section III focusses on control design and string stability analysis for CACC. Next, Section IV explains the test vehicle instrumentation, after which Section V presents experimental results, obtained with the test vehicles. Finally, Section VI summarizes the main conclusions and proposes directions for further research.

## II. STRING STABILITY REVIEW

Three main approaches of the notion of string stability can be distinguished, being a formal stability-like approach,

a stability approach for strings of infinite length, and finally a performance-oriented frequency-domain approach.

The formal stability-like approach is described in, e.g., [9], [11]. As opposed to system stability, which is essentially concerned with the evolution of system states over time, string stability focusses on the propagation of states over subsystems. Recently, new results appeared [12], regarding a one-vehicle look-ahead control architecture in a homogeneous string. These approaches employ common notions such as Lyapunov stability, input-output stability and input-to-state stability to devise a definition for string stability. They provide little support for controller synthesis, however.

Within the framework of string stability for infinite-length strings of identical interconnected subsystems, the model of such a system is formulated in the state space and subsequently transformed using the bilateral Z-transform [13], [14]. The Z-transform is executed over the vehicle index instead of over time, resulting in a model formulated in the “discrete frequency” domain, related to the vehicle index, as well as in the time domain. String stability can then be assessed by inspecting the eigenvalues of the state matrix. This method, although rather elegant, is however only applicable to linear, infinite-length strings.

Finally, a performance-oriented frequency-domain approach for string stability is frequently adopted since this appears to directly offer tools for controller synthesis [5], [7], [8], [10], [15]. Moreover, the fact that string stability in literature is commonly used as a performance objective rather than as a stability criterion, suggests an interpretation of string stability as such, despite its name. In the performance-oriented approach, string stability is characterized by the amplification in upstream direction of either distance error, velocity, or acceleration. This leads to the following definition, (implicitly) used in the above literature references.

**Definition 1 (Vehicle String Stability):** Consider a string of  $m \in \mathbb{N}$  interconnected vehicles. This system is string-stable if and only if

$$\|z_i(t)\|_{\mathcal{L}_p} \leq \|z_{i-1}(t)\|_{\mathcal{L}_p}, \quad \forall t \geq 0, 2 \leq i \leq m,$$

where  $z_i(t)$  can either be the distance error  $e_i(t)$ , the velocity  $v_i(t)$  or the acceleration  $a_i(t)$  of vehicle  $i$ ;  $z_1(t) \in \mathcal{L}_p$  is a given input signal, and  $z_i(0) = 0$  for  $2 \leq i \leq m$ .

$\|\cdot\|_{\mathcal{L}_p}$  denotes the signal  $p$ -norm, whereas the vehicles in the string are enumerated  $i = 1, \dots, m$ , with  $i = 1$  indicating the lead vehicle. Definition 1 thus states that  $\|z_i(t)\|_{\mathcal{L}_p}$  must decrease in upstream direction. Note that in literature, the choice for the scalar signal  $z_i(t)$ , i.e., either distance error, velocity, or acceleration, seems rather arbitrary.

The above string stability definition can directly be used for string stability analysis and has a clear physical meaning, as illustrated in the next section. It seems therefore well motivated to adopt the performance-oriented approach when designing CACC systems.

### III. CONTROL DESIGN

An elegant method to arrive at a suitable controller for CACC is based on formulation of the error dynamics, as

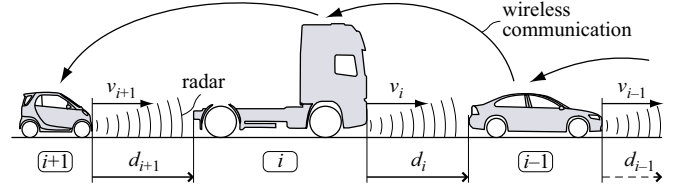


Fig. 2. CACC-equipped string of vehicles.

shown below. Having designed the controller, the string stability properties of the resulting closed-loop system are analyzed, using a condition that directly follows from Definition 1.

#### A. Error Dynamics

Consider a string of  $m$  vehicles, schematically depicted in Fig. 2, with  $d_i$  being the distance between vehicle  $i$  and its preceding vehicle  $i - 1$ , and  $v_i$  the velocity of vehicle  $i$ . The main objective of each vehicle is to follow its preceding vehicle at a desired distance  $d_{r,i}$ . Here, a constant time-headway spacing policy is adopted, formulated as

$$d_{r,i}(t) = r_i + hv_i(t), \quad 2 \leq i \leq m, \quad (1)$$

where  $h$  is the so-called time headway, and  $r_i$  is the standstill distance. This spacing policy is known to improve string stability [5], [8], [10], [12]. A homogeneous string is assumed, which is why the time headway  $h$  is taken independently of  $i$ . The spacing error  $e_i(t)$  is thus defined as

$$\begin{aligned} e_i(t) &= d_i(t) - d_{r,i}(t) \\ &= (s_{i-1}(t) - s_i(t) - L_i) - (r_i + hv_i(t)) \end{aligned} \quad (2)$$

with  $s_i(t)$  the position of vehicle  $i$  and  $L_i$  its length.

As a basis for control design, the following vehicle model is adopted:

$$\begin{pmatrix} \dot{d}_i \\ \dot{v}_i \\ \dot{a}_i \end{pmatrix} = \begin{pmatrix} v_{i-1} - v_i \\ a_i \\ -\frac{1}{\tau}a_i + \frac{1}{\tau}u_i \end{pmatrix}, \quad 2 \leq i \leq m, \quad (3)$$

where  $a_i$  is the acceleration of vehicle  $i$ ,  $u_i$  the external input, to be interpreted as desired acceleration, and  $\tau$  a time constant representing engine dynamics. This model is in fact obtained by formulating a more detailed model and then applying a pre-compensator, designed by means of input-output linearization by state feedback [7], [15]. Also note that the time constant  $\tau$  is assumed to be identical for all vehicles, corresponding to the above mentioned homogeneity assumption. With different types of vehicles in the string, as suggested by Fig. 2, homogeneity can be obtained by adequately designed pre-compensators so as to arrive at the vehicle behavior described by (3).

The control law can now be designed by formulating the error dynamics. Define to this end the error states

$$\begin{pmatrix} e_{1,i} \\ e_{2,i} \\ e_{3,i} \end{pmatrix} = \begin{pmatrix} e_i \\ \dot{e}_i \\ \ddot{e}_i \end{pmatrix}, \quad 2 \leq i \leq m. \quad (4)$$

Then, obviously,  $\dot{e}_{1,i} = e_{2,i}$  and  $\dot{e}_{2,i} = e_{3,i}$ . The third error state equation is obtained by differentiating  $e_{3,i} = \ddot{e}_i$ , while using (2) and (3), eventually resulting in:

$$\dot{e}_{3,i} = -\frac{1}{\tau}e_{3,i} - \frac{1}{\tau}q_i + \frac{1}{\tau}u_{i-1}, \quad (5)$$

with the new input

$$q_i \triangleq h\dot{u}_i + u_i. \quad (6)$$

From (5), it is immediately clear that the input  $q_i$  should stabilize the error dynamics while compensating for the input  $u_{i-1}$  of the preceding vehicle in order to obtain exact vehicle following, i.e.,  $\lim_{t \rightarrow \infty} |e_i(t)| = 0$ . Hence, the control law for  $q_i$  is designed as follows:

$$q_i = K \begin{pmatrix} e_{1,i} \\ e_{2,i} \\ e_{3,i} \end{pmatrix} + u_{i-1}, \quad 2 \leq i \leq m, \quad (7)$$

with  $K = (k_p \ k_d \ k_{dd})$ . Note that the feedforward term  $u_{i-1}$  is obtained through wireless communication with the preceding vehicle and, therefore, is the reason for the employment of a wireless communication link.

Due to the additional controller dynamics (6), the error dynamics must be extended with an additional equation, which can be obtained using the input definition (6) while substituting the control law (7):

$$\dot{u}_i = -\frac{1}{h}u_i + \frac{1}{h}(k_p e_{1,i} + k_d e_{2,i} + k_{dd} e_{3,i}) + \frac{1}{h}u_{i-1}. \quad (8)$$

As a result, the 4<sup>th</sup>-order closed-loop model reads

$$\begin{pmatrix} \dot{e}_{1,i} \\ \dot{e}_{2,i} \\ \dot{e}_{3,i} \\ \dot{u}_i \end{pmatrix} = \begin{pmatrix} 0 & 1 & 0 & 0 \\ 0 & 0 & 1 & 0 \\ -\frac{k_p}{\tau} & -\frac{k_d}{\tau} & -\frac{1+k_{dd}}{\tau} & 0 \\ \frac{k_p}{h} & \frac{k_d}{h} & \frac{k_{dd}}{h} & -\frac{1}{h} \end{pmatrix} \begin{pmatrix} e_{1,i} \\ e_{2,i} \\ e_{3,i} \\ u_i \end{pmatrix} + \begin{pmatrix} 0 \\ 0 \\ 0 \\ \frac{1}{h} \end{pmatrix} u_{i-1}. \quad (9)$$

Applying the Routh-Hurwitz stability criterion while using the fact that the state matrix in (9) is lower block-triangular, it follows that these error dynamics can be stabilized for any time headway  $h > 0$ , and with any choice for  $k_p, k_d > 0$ ,  $k_{dd} > -1$ , such that  $(1 + k_{dd})k_d > k_p\tau$ . Note that the stability of the dynamics (9) is sometimes referred to as *individual vehicle stability* [8], [9].

### B. String Stability Analysis

Under the conditions stated above, the controller (7) thus realizes the vehicle following objective, but does not yet guarantee string stability. In order to analyze the latter, a string stability criterion is derived first. Introduce to this end the *string stability complementary sensitivity*  $\Gamma_i(s)$ , being the transfer function from “input” velocity  $\hat{v}_{i-1}(s)$  to “output” velocity  $\hat{v}_i(s)$ , i.e.,

$$\hat{v}_i(s) = \Gamma_i(s)\hat{v}_{i-1}(s), \quad 2 \leq i \leq m, \quad (10)$$

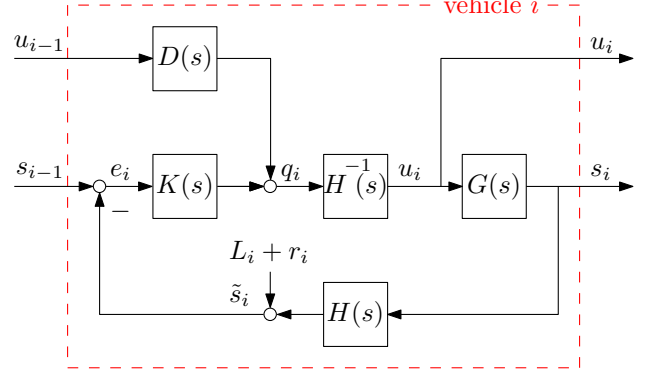


Fig. 3. Block scheme of the CACC system.

where  $\hat{v}(s)$ , with  $s \in \mathbb{C}$ , denotes the Laplace transform of  $v(t)$ . Here, the velocity is taken as a basis for string stability, which is more relevant than distance error in view of traffic analysis [3]. Note that the choice between velocity or acceleration is irrelevant, since  $\Gamma_i(s)$  is identical in both cases. Taking  $p = 2$ , the following relation from linear system theory holds:

$$\|\Gamma_i(j\omega)\|_{\mathcal{H}_\infty} = \max_{v_{i-1} \neq 0} \frac{\|v_i(t)\|_{\mathcal{L}_2}}{\|v_{i-1}(t)\|_{\mathcal{L}_2}}, \quad (11)$$

where  $\Gamma_i(j\omega)$  is the transfer function evaluated along the imaginary axis.  $\|\cdot\|_{\mathcal{H}_\infty}$  denotes the  $\mathcal{H}_\infty$  norm, which, for scalar transfer functions, equals the supremum of  $|\Gamma_i(j\omega)|$  over the frequency  $\omega$ . Using (11), Definition 1 immediately leads to the following string stability condition:

$$\|\Gamma_i(j\omega)\|_{\mathcal{H}_\infty} \leq 1, \quad 2 \leq i \leq m. \quad (12)$$

This condition can be interpreted as requiring energy dissipation in upstream direction. This follows from the fact that, according to (11), the  $\mathcal{H}_\infty$  norm is induced by the  $\mathcal{L}_2$  norms of input and output, which, in turn, are measures for energy.

According to (12), string stability is thus assessed in the frequency domain. Introduce to this end the vehicle transfer function  $G(s) = \hat{s}_i(s)/\hat{u}_i(s)$ :

$$G(s) = \frac{1}{s^2(\tau s + 1)}, \quad (13)$$

which follows from the fact that  $\ddot{s}_i = -\frac{1}{\tau}\dot{s}_i + \frac{1}{\tau}u_i$ , see (3). Also introduce the *spacing policy transfer function*  $H(s) = \hat{q}_i(s)/\hat{u}_i(s)$ , derived from (6):

$$H(s) = hs + 1, \quad (14)$$

and the feed law  $K(s) = \hat{q}_i(s)/\hat{e}_i(s)$ , defined in (7):

$$K(s) = k_p + k_{d1}s + k_{d2}s^2. \quad (15)$$

The controlled vehicle can then be represented by the block scheme depicted in Fig. 3. The occurrence of the spacing policy transfer function  $H(s)$  in the feedback loop can be readily explained. Considering  $\tilde{s}_i$ , as depicted in the block scheme, it appears that, using (14),

$$\tilde{s}_i(t) = L_i + r_i + s_i(t) + hv_i(t). \quad (16)$$

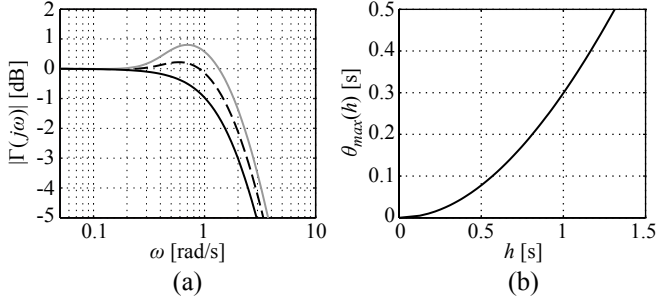


Fig. 4. String stability properties: (a) string stability complementary sensitivity  $|\Gamma(j\omega)|$  for communication delay (solid black)  $\theta = 0$  s, (dashed black)  $\theta = 0.15$  s, and (solid grey)  $\theta = 0.3$  s, and (b) maximum string stable communication delay  $\theta_{max}(h)$ .

Hence,  $\tilde{s}_i$  can be interpreted as the “virtual control point” of vehicle  $i$ , that must be as close as possible to the actual position  $s_{i-1}$  of the preceding vehicle  $i - 1$ .

The block scheme also includes a time delay  $D(s) = e^{-\theta s}$ , representing the latency  $\theta$  induced by the wireless communication network due to queueing, contention, transmission, and propagation. This delay can only be compensated for by means of an estimator, which is, however, considered out-of-scope for this paper. Using this block scheme,  $\Gamma_i(s) = \Gamma(s)$  (independent of  $i$ ) can be shown to be equal to

$$\Gamma(s) = \frac{1}{H(s)} \frac{D(s) + G(s)K(s)}{1 + G(s)K(s)}. \quad (17)$$

According to (10),  $\Gamma(s)$  is the transfer function from  $v_{i-1}$  to  $v_i$ . Surprisingly, when taking the distance errors  $e_{i-1}$  and  $e_i$  instead,  $\Gamma(s)$  appears to be identical. This is due to the homogeneity assumption.

The communication delay plays an important role with respect to string stability. Without delay, i.e.,  $D(s) = 1$ , the controlled system is string stable by definition, since  $\|\Gamma(j\omega)\|_{\mathcal{H}_\infty} = \sup_{\omega} |H^{-1}(j\omega)| = 1$ . Note that, due to the vehicle following objective,  $\|\Gamma(j\omega)\|_{\mathcal{H}_\infty}$  will never be smaller than 1. However, the existence of a communication delay compromises string stability to a certain extent, as illustrated in Fig. 4. Using  $\tau = 0.1$  s,  $k_p = 0.2$ ,  $k_d = 0.7$ ,  $k_{dd} = 0$  (refer to Section V), and time headway  $h = 0.5$  s, Fig. 4(a) shows the gain  $|\Gamma(j\omega)|$  for various values of the time delay  $\theta$ . It appears that an increasing time delay yields an increased value of  $\|\Gamma(j\omega)\|_{\mathcal{H}_\infty}$ .

From (17) also follows that increasing the time headway  $h$  decreases  $\|\Gamma(j\omega)\|_{\mathcal{H}_\infty}$ , in the case of a non-zero delay  $\theta$ . This is illustrated in Fig. 4(b), showing the maximum communication delay  $\theta_{max}$  that yields string stability, as a function of headway time  $h$ . The curve shown here is calculated iteratively by taking a fixed value for  $\theta$  and then searching for the value of  $h$  such that  $\|\Gamma(j\omega)\|_{\mathcal{H}_\infty} = 1$ . From this figure, it can be inferred that a vehicle string with  $h = 0.5$  s would require  $\theta$  to be smaller than about 80 ms in view of string stability.

Note that, in practice, the controller and the wireless communication are implemented in discrete-time, which may

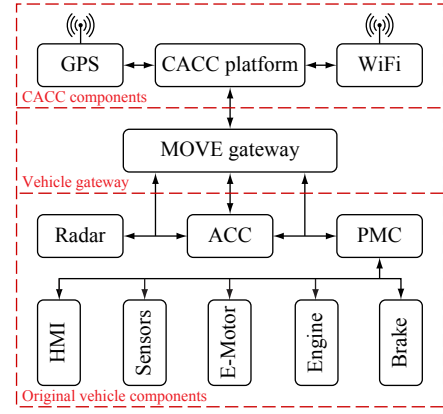


Fig. 5. Schematic representation of the test vehicle instrumentation.

affect string stability as well [16]. Assuming a sufficiently high sampling frequency, these effects are ignored here.

Finally, it is worth mentioning that the string stability complementary sensitivity in case of ACC can be easily obtained from (17) by choosing  $D(s) = 0$ . As a result, ACC appears to be string stable for  $h \geq 3.16$  s, given the above mentioned model and controller parameters.

#### IV. VEHICLE INSTRUMENTATION

In order to validate the theoretical results and to demonstrate the technical feasibility, the CACC control system has been implemented in six similarly adapted vehicles. The Toyota Prius III Executive was selected because of its modular setup and ex-factory ACC. Fig. 5 shows a schematic representation of the components related to the experimental setup. From this figure, it appears that the CACC-related components can be categorized into original vehicle components, CACC-specific components, and the vehicle gateway. These three groups are subsequently explained below.

By making use of many original vehicle systems, only a limited number of components had to be added. The long-range radar determines the relative position and speed of multiple objects with an update rate of 20 Hz. The ESP sensor cluster measures acceleration in two directions, as well as yaw rate. The Power Management Control (PMC) determines the setpoints for the electric motor, the hydraulic brakes, and the engine. Finally, the Human-Machine Interface (HMI) consists of levers and a display.

Some CACC-specific components had to be implemented in the vehicle in order to run the CACC system properly. The main component is a real-time computer platform that executes the CACC control functionality. The WiFi device, operating according to the IEEE 802.11a standard in ad-hoc mode, allows for communication of the vehicle motion and controller information between the CACC vehicles with an update rate of 10 Hz. A GPS receiver, with an update rate of 1 Hz, has been installed to allow for synchronization of measurement data using its time stamp.

Finally, the in-house developed MOVE gateway is the interface between the original vehicle systems and the real-time CACC platform. It runs at 100 Hz, converting the



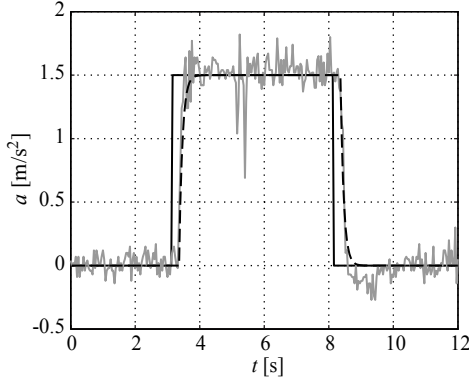


Fig. 6. Step response of the test vehicle with low-level control only: (solid black) desired acceleration, (dashed black) simulated acceleration, (solid grey) measured acceleration.

acceleration setpoints  $u_i$  from the CACC platform, into vehicle actuator setpoints, such that the requested acceleration is accurately realized. The gateway also processes the vehicle sensor data and presents these to the CACC platform. Furthermore, the gateway is connected to the vehicle HMI (digital display and levers). As a result, the CACC can be operated like the ex-factory ACC system. To guarantee safe and reliable operation, the gateway also contains several safety features. The gateway employs multiple I/O for the communication with the vehicle systems; a single CAN bus is used for communication with the CACC platform.

Because of the integrated low-level controllers, safety-related functions, and sensor preprocessing, the MOVE gateway allows for evaluation of high-level vehicle controllers, such as CACC, in a safe, reliable and efficient way.

## V. PRACTICAL EXPERIMENTS

To validate the designed controller, experiments are performed using the test fleet. To this end, the vehicle model is identified first, based on which the controller parameters are chosen. Next, ACC as well as CACC are evaluated to compare the performance of both control systems.

### A. Vehicle Model Validation

The vehicle model, including a low-level pre-compensator implemented in the MOVE gateway, is identified based on measurement of the response of the acceleration  $a(t)$  to test signals applied to the desired acceleration  $u(t) = a_{ref}(t)$ . Subsequently, the model parameters are estimated using a least-squares method. From this, it appears that the vehicle model (3) needs to be adapted so as to include a time delay  $\phi$ , having the following frequency-domain model as a result:

$$G(s) = \frac{1}{s^2(\tau s + 1)} e^{-\phi s} \quad (18)$$

with  $\tau = 0.1$  s and  $\phi = 0.2$  s.

Fig. 6 illustrates a validation measurement, showing the test signal  $a_{ref}(t)$ , and the measured as well as the simulated acceleration  $a(t)$  using the identified parameters. It can be concluded that the simple vehicle model adequately describes the longitudinal vehicle dynamics; it is fair to mention that

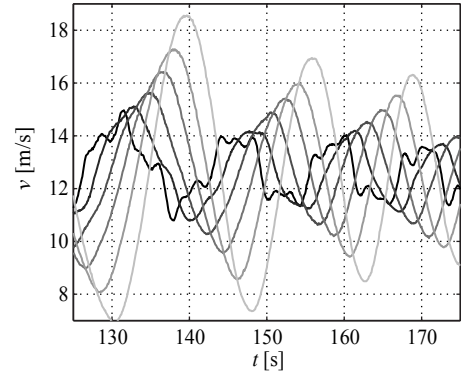


Fig. 7. Measured ACC velocity response: (black–light grey) vehicle 1–6.

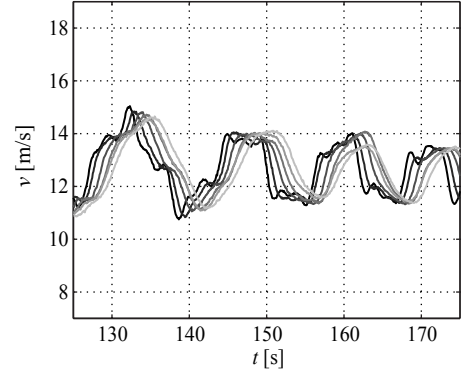


Fig. 8. Measured CACC velocity response: (black–light grey) vehicle 1–6.

the well-designed drive train of the test vehicles highly contributes to this result. Obviously, this longitudinal model does not hold for limit situations, characterized by nonlinear behavior due to tire slip or power limitations, for instance.

Based on speed of response and passenger comfort, suitable controller parameters were found to be  $k_p = 0.2$  and  $k_d = 0.7$ , whereas  $k_{dd}$  is set to zero to prevent feedback of the vehicle's jerk, which is in practice unfeasible.

### B. String Stability Experiments

The wireless communication delay in the current test set-up equals  $\theta \approx 150$  ms. From the theory presented in Section III, it follows that for this delay, and with the above vehicle and controller parameters, the minimum necessary time headway for string stability equals  $h_{min} = 0.67$  s. Therefore, tests have been performed with  $h = 0.7$  s.

The test trajectory is defined by the desired acceleration  $a_{ref,1}(t)$  of the lead vehicle, and consists of three superimposed swept sine signals in the frequency ranges  $[0.06, 1.13]$  rad/s,  $[1.13, 2.26]$  rad/s, and  $[2.26, 3.14]$  rad/s, respectively. In view of a high level of reproducibility, the lead vehicle is not manually driven, but instead has been equipped with a velocity controller. The desired velocity  $v_{ref,1}(t)$  is determined through integration of  $a_{ref,1}(t)$ , while using the latter as a feedforward signal.

Fig. 7 and Fig. 8 illustrate the test results for an ACC set-up and for CACC, respectively. Here, the ACC controller is simply obtained by disabling the input feedforward, i.e.,

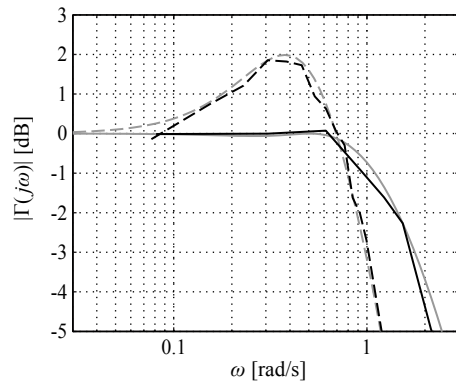


Fig. 9. String stability complementary sensitivity  $|\Gamma(j\omega)|$ : (solid grey) CACC, simulated, (solid black) CACC, measured, (dashed grey) ACC, simulated, (dashed black) ACC, measured.

omitting  $u_{i-1}$  in (7). Both figures show the velocity responses of all six vehicles for part of the test trajectory, where the velocity response of the lead vehicle is exactly the same since this vehicle is velocity controlled. It can be clearly seen that the CACC response is string stable, whereas the ACC response is not, which corresponds to the theoretical analysis. Noteworthy is the fast increase in overshoot for increasing vehicle index in case of ACC: the maximum velocity (in the time interval shown) of the last vehicle equals 18.6 m/s (67 km/h), whereas for CACC, this is 14.6 m/s (53 km/h).

The specific test trajectory, consisting of superimposed swept sines, provides sufficient frequency content to allow for identification of the string stability complementary sensitivity  $\Gamma(j\omega)$ . Using a non-parametric system identification method, the gain  $|\Gamma(j\omega)|$  has been estimated, the result of which is shown in Fig. 9. This figure shows the estimated gain  $|\Gamma(j\omega)|$  for both ACC and CACC, as well as the theoretical gain, calculated using (17). This not only confirms the string stability properties of both controllers, but also validates the theoretical analysis presented in Section III.

## VI. CONCLUSIONS AND FUTURE WORK

String stability is an essential requirement for the design of vehicle following control systems that aim for short-distance following. It has been shown, theoretically and experimentally, that Cooperative Adaptive Cruise Control (CACC), which is based on common ACC sensors and a wireless inter-vehicle communication link, allows for time gaps significantly smaller than 1 s while maintaining string stability. In the experimental set-up, consisting of a test fleet of six vehicles, a time headway of 0.7 s appeared to yield string-stable behavior. This result fully corresponds to the theoretical analysis, which also indicates that time gaps less than 0.5 s are feasible when optimizing the wireless link with respect to latency. As a result, a significant increase in road throughput and, in case of heavy-duty vehicles, decrease of fuel consumption and emissions can be expected. Moreover, the experimental set-up also illustrated that this functionality can be obtained by very limited adaptations to the existing vehicle, provided it has already been equipped with ACC.

Finally, the CACC controller does not require numerically intensive computations and should, therefore, be suitable to implement in the existing embedded vehicle control systems.

Current developments are focussing on implementation aspects such as fail safety. Driving at small time gaps requires a CACC system that is highly reliable and, if it fails, will do so gracefully. Also, the topic of object tracking is of main importance. In complex environments, imposed by everyday road traffic, radar information needs to be matched to the corresponding wireless information and, if necessary, sensor fusion algorithms to obtain reliable object information need to be employed.

## REFERENCES

- [1] A. Vahidi and A. Eskandarian, "Research advances in intelligent collision avoidance and adaptive cruise control," *IEEE Trans. Intell. Transp. Syst.*, vol. 4, no. 3, pp. 143–153, Sept. 2003.
- [2] *Transport information and control systems – Adaptive Cruise Control systems – Performance requirements and test procedures*, International Organization for Standardization Std. ISO 15 622, Oct. 2002.
- [3] B. van Arem, C. J. G. van Driel, and R. Visser, "The impact of cooperative adaptive cruise control on traffic-flow characteristics," *IEEE Trans. Intell. Transp. Syst.*, vol. 7, no. 4, pp. 429–436, Dec. 2006.
- [4] S. E. Shladover, "Automated vehicles for highway operation (automated highway systems)," *Proceedings of the Institution of Mechanical Engineers, Part I: Journal of Systems and Control Engineering*, vol. 219, no. 1, pp. 53–75, 2005.
- [5] G. J. L. Naus, R. P. A. Vugts, J. Ploeg, M. J. G. van de Molengraft, and M. Steinbuch, "String-stable CACC design and experimental validation: A frequency-domain approach," *IEEE Trans. Veh. Technol.*, vol. 59, no. 9, pp. 4268–4279, Nov. 2010.
- [6] W. S. Levine and M. Athans, "On the optimal error regulation of a string of moving vehicles," *IEEE Trans. Autom. Control*, vol. 11, no. 3, pp. 355–361, July 1966.
- [7] S. Sheikholeslam and C. A. Desoer, "Longitudinal control of a platoon of vehicles with no communication of lead vehicle information: A system level study," *IEEE Trans. Veh. Technol.*, vol. 42, no. 4, pp. 546–554, Nov. 1993.
- [8] O. Gehring and H. Fritz, "Practical results of a longitudinal control concept for truck platooning with vehicle to vehicle communication," in *Proceedings of the IEEE Conference on Intelligent Transportation Systems*, Nov. 9–12 1997, pp. 117–122.
- [9] D. Swaroop and J. K. Hedrick, "Constant spacing strategies for platooning in automated highway systems," *ASME Journal of Dynamic Systems, Measurement, and Control*, vol. 121, no. 3, pp. 462–470, Sept. 1999.
- [10] R. Rajamani and C. Zhu, "Semi-autonomous adaptive cruise control systems," *IEEE Trans. Veh. Technol.*, vol. 51, no. 5, pp. 1186–1192, Sept. 2002.
- [11] D. Swaroop and J. K. Hedrick, "String stability of interconnected systems," *IEEE Trans. Autom. Control*, vol. 41, no. 3, pp. 349–357, Mar. 1996.
- [12] S. Klinge and R. H. Middleton, "String stability analysis of homogeneous linear unidirectionally connected systems with nonzero initial conditions," in *Proceedings of the IET Irish Signals and Systems Conference*, June 11–12 2009.
- [13] M. L. El-Sayed and P. S. Krishnaprasad, "Homogeneous interconnected systems: An example," *IEEE Trans. Autom. Control*, vol. 26, no. 4, pp. 894–901, Aug. 1981.
- [14] E. Barbieri, "Stability analysis of a class of interconnected systems," *ASME Journal of Dynamic Systems, Measurement, and Control*, vol. 115, no. 3, pp. 546–551, Sept. 1993.
- [15] S. S. Stanković, M. J. Stanojević, and D. D. Šiljak, "Decentralized overlapping control of a platoon of vehicles," *IEEE Trans. Control Syst. Technol.*, vol. 8, no. 5, pp. 816–832, Sept. 2000.
- [16] S. Öncü, N. van de Wouw, and H. Nijmeijer, "Cooperative adaptive cruise control: Tradeoffs between control and network specifications," *Submitted to the IEEE Conference on Intelligent Transportation Systems*, Washington D.C., USA, Oct. 5–7 2011.